Mapping the Bimolecular Interface of the Parathyroid Hormone (PTH)−PTH1 Receptor Complex: Spatial Proximity between Lys^{27} (of the Hormone Principal Binding Domain) and Leu^{261} (of the First Extracellular Loop) of the Human PTH1 Receptor†

Zvi Greenberg, Alessandro Bisello, Dale F. Mierke,‡ Michael Rosenblatt, and Michael Chorev*

Division of Bone and Mineral Metabolism, Charles A. Dana and Thorndike Laboratories, Department of Medicine, Beth Israel Deaconess Medical Center and Harvard Medical School, Boston, Massachusetts 02215, and the Department of Molecular Pharmacology, Physiology and Biotechnology, Division of Biology and Medicine, and the Department of Chemistry, Brown University, Providence, Rhode Island 02912

Received February 1, 2000; Revised Manuscript Received May 1, 2000

ABSTRACT: In an effort to characterize the bimolecular interface between parathyroid hormone (PTH) and its human receptor PTH1-Rc (hPTH1-Rc), we previously identified two contact sites in the receptor: one for position 1 and another for position 13 (located at the ends of the principal activation domain) in PTH(1−34). The present study reports a third, novel "contact site" between hPTH1-Rc and Lys^{27} of PTH(1−34). Lys^{27} is located in the principal binding domain of the hormone (residues 25−34). The photoreactive PTH(1−34) analogue K27 contains a benzophenone (BP) moiety on Lys^{27}. The analogue binds to stably transfected HEK 293/C-21 cells (which express a high level of recombinant hPTH1-Rc) and stimulates adenylyl cyclase activity with a potency similar to PTH(1−34). In addition, ^{125}I-K27 cross-links effectively and specifically to the hPTH1-Rc. Enzymatic (Glu-C and Lys-C) and chemical (CNBr and BNPS-skatole) digestions of the photoconjugate between ^{125}I-K27 and hPTH1-Rc were performed. In addition, photoconjugates involving the bioactive mutants [L261M]- and [R262K]-hPTH1-Rc, transiently expressed in COS-7 cells, were also digested. The data obtained clearly identify L^{261} or R^{262} of the first extracellular loop of hPTH1-Rc as the contact site for Lys^{27} in the hormone. On the basis of (i) the similarity in molecular mass between the CNBr digest of the ^{125}I-K27−[L261M]hPTH1-Rc conjugate and free ^{125}I-K27 and (ii) the failure to cross-link ^{125}I-K27 to a bioactive mutant receptor [L261A]hPTH1-Rc, we conclude that L^{261} is the cross-linking site. These results provide the first demonstration of an interaction between the principal binding domain of PTH and the first extracellular loop of hPTH1-Rc. Revealing proximity of Lys^{27} (in PTH) to L^{261} (in hPTH1-Rc) provides additional insight into the nature of the ligand−receptor bimolecular interface and clearly illustrates that the extracellular loops of the receptor contribute to the specificity of the PTH−PTH1-Rc interaction. Taken together with previous studies, the new findings add important constraints on the possible positioning of the C-terminal helix of PTH (which contains the principal binding domain) relative to the first extracellular loop and the distal C-terminal helix of the large extracellular amino terminal domain of the PTH1-Rc.

Parathyroid hormone (PTH)[1] is the major hormone responsible for the regulation of blood calcium levels and is involved in bone remodeling (*1*). The hormone exerts these activities via a seven transmembrane domain-containing G-protein-coupled receptor (PTH1-Rc) (*2*), which is a member of the glucagon/secretin/calcitonin/vasoactive intestinal peptide receptor subfamily (*3*, *4*). Activation of PTH1-Rc triggers intracellular signaling via both the adenylyl cyclase/cAMP/protein kinase A and phospholipase C/inositol-(1,4,5)-triphosphate (IP_3)/intracellular Ca^{2+} pathways (*5*−*8*). Interestingly, PTH(1−34), the N-terminal sequence of PTH, effectively displays the full scope of PTH-like calciotropic activities (*9*). Elucidating the nature of the bimolecular interaction between PTH and PTH1-Rc is essential for understanding the molecular mechanisms involved in ligand-specific recognition, binding, and receptor activation.

† This work was supported by NIH Grant RO1-DK47940 (to M.R.).

* To whom correspondence should be addressed at Division of Bone & Mineral Metabolism (HIM 944), Beth Israel Deaconess Medical Center, Harvard Medical School, 330 Brookline Avenue, Boston, MA 02215. Telephone: 617-667-0901; fax: 617-667-4432; e-mail: michael_chorev@hms.harvard.edu.

‡ Brown University.

[1] Abbreviations: Boc, *tert*-butyloxycarbonyl; BP, benzophenone; DCC, *N*,*N*′-dicyclohexylcarbodiimide; D-MEM, Dulbecco's modified Eagle's medium; ECD, extracellular domain; ECL, extracellular loop; EDTA, ethylenediaminetetraacetic acid; Endo-F, endoglycosidase F/N-glycosidase F; FBS, fetal bovine serum; Fmoc, 9-fluorenylmethyloxycarbonyl; HEK, human embryonic kidney; hPTH1-Rc, type 1 human PTH receptor; HOBt, *N*-hydroxybenzotriazole; IBMX, 3-isobutyl-1-methylxantine; ICL, intracellular loop; K27, [Nle^{8,18}, Arg^{13,26}, L-2-Nal^{23}, Lys^{27}(N$^{\epsilon}$-*p*Bz$_2$), Tyr^{34}]bPTH(1−34)NH$_2$; Lys-C, lysyl endopeptidase; Nal, naphthylalanyl; NMP, *N*-methylpyrrolidone; PAGE, polyacrylamide gel electrophoresis; PAS, photoaffinity scanning; PBS, phosphate-buffered saline; *p*Bz$_2$, *para*-benzoylbenzoyl; PTH, parathyroid hormone; PTH(1−34), [Nle^{8,18}, Tyr^{34}]bPTH(1−34)NH$_2$; RP-HPLC, reversed-phase high performance liquid chromatography; rt, room temperature; SDS, sodium dodecylsulphate; TB, total binding; TM, transmembrane domain; wt, wild-type.

10.1021/bi000195n CCC: $19.00
Published on Web 06/21/2000

The photoaffinity scanning (PAS) approach, initially reported by Williams and Shoelson (*10*), takes advantage of the unique photochemical properties of the benzophenone (BP) moiety as a photophore (*11*) to probe the bimolecular interface between a ligand and a macromolecular acceptor. In the absence of solution or solid-state structures of ligand−G-protein-coupled receptor complexes, PAS is the only direct approach to studying ligand−receptor bimolecular interactions. As such, it complements and enhances the more commonly used structure−activity-based strategies, in which indirect reporters of the nature of ligand−receptor interactions, such as the biological activities of structurally modified ligands and/or receptors, form the sole basis for insight into hormone−receptor interactions. The PAS approach has been utilized in the characterization of peptide ligand−receptor systems, including substance-P, vasopressin, luteinizing hormone, and natriuretic peptide (*12*−*19*). The basic premise on which PAS operates is that the photophore-modified ligand binds to the target acceptor in a similar fashion as nonmodified ligand, namely, with high affinity, and induces the same profile of bioactivities. Therefore, especially in the case of BP as the photophore, the insertion site may represent either an actual contact point between ligand and receptor or a site in the immediate spatial proximity of such a contact point. With that in mind, our use of the term "contact point" or "contact site" has its obvious limitations that are operationally defined.

The present study is part of an ongoing PAS effort directed at identifying distinct sites within the hPTH1-Rc that are in proximity to specific residues in PTH(1−34). To this end, we developed bioactive, radioiodine-tagged, singularly BP-substituted PTH(1−34) analogues resistant to specific enzymatic and chemical digestions. These analogues are photocross-linked to recombinant hPTH1-Rc stably expressed in high levels (400 000 Rcs/cell) in human embryonic kidney (HEK) 293/C-21 cells, which provide a species homologous cellular background (*7*). Radiolabeled conjugated fragments are then generated using a series of specific chemical and enzymatic digestions of the radiolabeled PTH−PTH1-Rc photoconjugate. These fragments are used to identify the putative photoinsertion site of ligand into receptor by comparing their electrophoretically derived apparent molecular weights with the theoretical cleavage-specific digestion map of the hPTH1-Rc sequence. The contact sites identified with the wild-type hPTH1-Rc are validated and further delineated employing a series of fully active, transiently expressed site-directed mutants of the hPTH1-Rcs (*20*−*24*). The contact sites thus identified are used as structural constraints in the molecular modeling of the ligand−receptor complex.

Utilizing this strategy (*25*), contact sites in hPTH1-Rc for residues 1 and 13, located in the activation domain of PTH, have been identified (*20*, *24*, *26*). The N-terminal residue (position 1) in PTH(1−34) cross-links to M[425] located[2] in transmembrane domain (TM) 6, close to the third extracellular loop (ECL) of the receptor (*20*). Lys[13] of the hormone cross-links to a site in the proximity of R[186], which is located at the junction of the N-terminal extracellular domain and TM1 of hPTH1-Rc (*24*, *26*). The identification of these contact sites played a major role in the construction of the first experimentally derived model of the PTH(1−34)−PTH1-Rc complex (*20*, *27*).

Here we report our efforts to identify for the first time the contact site between a portion of the "principal binding domain" of PTH, amino acid residues 25−34 (*25*, *28*), and the recombinant hPTH1-Rc. We now identify L[261] in ECL1 of the hPTH1-Rc as the contact site for Lys[27] in PTH(1−34). In the following paper in this issue, the conformational features of ECL1 of hPTH1-Rc, as determined by high-resolution NMR and molecular calculations, are detailed and provide structural insight into the relative spatial orientation of the hormone and portions of the receptor (*29*). Our analysis supports a specific intermolecular topological arrangement in which the C-terminal helix of PTH is located between the ECL1 and the distal C-terminal helix of the large extracellular amino terminal domain of PTH1-Rc.

EXPERIMENTAL PROCEDURES

Materials. Boc-protected amino acids, *N*-hydroxybenzotriazole (HOBt), *N*,*N*′-dicyclohexylcarbodiimide (DCC), and *p*-methylbenzhydrylamine resin were purchased from Applied Biosystems (Foster City, CA). B&J brand dichloromethane, *N*-methylpyrrolidone (NMP), and acetonitrile were obtained from Baxter (McGraw Park, IL). IODOGEN and 2-(2′-nitrophenylsulfenyl)-3-methyl-3-bromoindolenine (BNPS-skatole) from Pierce Chemical Co. (Rockford, IL). Cyanogen bromide (CNBr) and Vydac 218TP C_{18} silica were from Aldrich (Milwaukee, WI). [^{125}I]Na was from Amersham Pharmacia Biotech. (Arlington Heights, IL). Endoglycosidase F/N-glycosidase F (Endo-F), Lysyl endopeptidase (Lys-C), and FuGENE 6 transfection reagent were purchased from Boehringer Mannheim (Indianapolis, IN). D-MEM, fetal bovine serum, Opti-MemI, and PBS were from Life Technologies, Inc. Tissue culture disposables and plasticware were obtained from Corning (Corning, NY). All other reagents were purchased from Sigma (St. Louis, MO). COS-7 cells were a generous gift of Dr. Steven Goldring, Beth Israel Deaconess Medical Center (Boston, MA).

Peptide Synthesis. [Nle[8,18], Tyr[34]]bPTH(1−34)NH_2 [PTH(1−34)] and [Nle[8,18], Arg[13,26], L-2-Nal[23], Lys[27](N$^{\epsilon}$-*p*Bz$_2$), Tyr[34]]bPTH(1−34)NH_2 (K27) were synthesized by the solid-phase methodology (*30*) on an Applied Biosystems 430A peptide synthesizer using Boc/HOBt/NMP chemistry. Detailed protocols for the synthesis, purification, and characterization of peptides are reported elsewhere (*20*, *26*, *31*, *32*). During synthesis of the K27 analogue Lys[27] was introduced as the N$^{\alpha}$-Boc-Lys(N$^{\epsilon}$-Fmoc)-OH derivative. After incorporation, the N$^{\epsilon}$-Fmoc protecting group was removed by two consecutive treatments for 5 and 40 min with 20% piperidine in NMP. Four equivalents of 4-benzoylbenzoic acid were then coupled in the presence of HOBt and DCC in NMP for 2 h followed by the standard solid-phase peptide synthesis as described above. After hydrogen fluoride cleavage, the peptides were purified by preparative reversed-phase high performance liquid chromatography (RP-HPLC). Purity exceeded 97% as determined by analytical RP-HPLC. Structural integrity of the peptides was confirmed by amino acid analysis and electrospray mass spectrometry.

[2] To simplify the reference to amino acid residues in the ligand and the receptor, the amino acids of the ligand are denoted using the three-letter code, while the one-letter notation is used for the residues of the receptor.

Radioiodinations. K-27 and PTH(1−34) were radioiodinated, and the crude radioiodinated material was purified as previously described (*33*). Briefly, 67 μg of peptide in 50 μL of phosphate buffer, pH 7.4, in a borosilicate tube, coated with 10 μg of Iodogen, was treated with 2 mCi [^{125}I]Na for 12 min, followed by dilution with 200 μL of 0.1% trifluoroacetic acid (TFA) in water. The crude mono-radioiodinated peptide was isolated on an analytical RP-HPLC Vydac Protein C18 column (The Separation Group, Hesparia, CA) employing a linear gradient of 36−42% B in A for 30 min (A = 0.1% TFA in water; B = 0.1% TFA in acetonitrile) at a flow rate of 1 mL/min and monitored at 220 nm.

Cell Cultures. HEK-293 cells stably transfected with hPTH1-Rc (clone C-21, ∼400 000 receptors/cell) (*7*) and COS-7 cells were maintained in D-MEM supplemented with 10% FBS. The cells were incubated at 37 °C in the presence of 5% CO_2 in humidified air.

Binding Assay. Cells were plated in 24-well tissue culture dishes (Corning, NY) and grown to subconfluency. The cells were then incubated for 2 h at room temperature in fresh FBS supplemented medium (0.25 mL) containing 100 000 cpm (∼0.1 nM) radioiodinated ligand (^{125}I-PTH(1−34) or ^{125}I-K27) in the presence or absence of increasing concentrations of unlabeled competing ligand. Following incubation, cells were washed twice with phosphate buffered saline (PBS) and lysed with 0.1 M NaOH. Radioactivity in the lysate was measured in a γ-counter (TmAnalytic GammaTrac 1193).

Adenylyl Cyclase Activation Assay. Stimulation of adenylyl cyclase activity by the PTH(1−34) analogues was assayed in stably transfected HEK293/C21 and transiently transfected COS-7 cells as described before (*31*). Shortly, cells were grown to confluency in 24-well culture dishes. They were then incubated with 0.5 μCi [^{3}H]adenine in fresh FBS supplemented medium at 37 °C for 2 h and further treated with 1 mM 3-isobutyl-1-methylxantine (IBMX) in fresh medium for 15 min at 37 °C. This treatment was followed by a 5-min incubation with the corresponding analogue. The reaction was terminated by adding 1.2 M trichloroacetic acid and neutralized with 4 N KOH. cAMP was isolated by the two-column chromatographic method (*34*). Radioactivity was measured in a scintillation counter (Beckman LS6000IC liquid scintillation counter, Downers Grove, IL).

Photoaffinity Labeling. Mini-scale: for the initial assessment of cross-linking effectiveness and specificity, cells were cultured to confluency in 24-well tissue culture dishes and washed twice with PBS. The cells were then incubated at room temperature for 15 min in 225 μL of D-MEM in the absence or presence of cold ligand (1 μM) and for an additional 30 min with ^{125}I-K27 (1×10^6 cpm, ∼1 nM) in a total volume of 250 μL. For photocross-linking, the uncovered dishes were placed on ice at a 10-cm distance from six 15-W, 365-nm UV lamps in a Stratalinker 2400 (Stratagene) and irradiated for 30 min. The cells were washed twice with PBS and lysed by shaking in Laemmli sample buffer (300 μL) for 30 min (*35*). Fifty microliters of the lysate was analyzed by 7.5% SDS−PAGE.

Preparative scale: for extraction of radiolabeled ligand−receptor conjugates, the cells were grown to confluency in 10-cm tissue culture dishes, harvested using EDTA, washed 4 times with PBS, and resuspended in D-MEM (11 mL). Following the addition of ^{125}I-K27 (1 mL, 0.2 mCi, ∼10 nM), the cell suspension was aliquoted into a 6-well plate (2.3×10^7 cells/well). The radioactive suspension was incubated for 60 min at room temperature and irradiated at 365 nm for 60 min as described above. Cells were collected into a 50-mL plastic tube (Falcon) and washed 5−6 times with PBS (centrifuged at 1000 rpm).

Receptor Extraction. The pellet of radiolabeled cross-linked cells was resuspended in 25 mM Tris-HCl buffer, pH 8.5 (12 mL), lysed by 5−6 freeze/thaw cycles, and the lysate was centrifuged at 900*g* for 20 min. Cell membranes were pelleted by ultracentrifugation of the supernatant at 10^5*g* for 2 h at 4 °C. For receptor extraction, the membrane pellet was subjected to end-over-end shaking in extraction buffer (25 mM Tris-HCl, 100 mM dithiotreitol, 2% Triton X-100, and 0.02% (w/v) sodium azide, pH 8.5; 200 μL/tube) for 16 h at room temperature followed by 30 min centrifugation at 2000*g*. Membrane proteins were extracted by incubating the supernatant with 5 supernatant vol of cold acetone for 16 h at −20 °C and collected by centrifugation (250*g*, 30 min). The pellet was redissolved 2% (w/v) SDS in water. Proteins were reduced with 100 mM dithiotreitol for 1 h at 37 °C and alkylated with 200 mM iodoacetamide for 15 min at room temperature. The solution was desalted and concentrated on Centricon 50 microconcentrators (Amicon), diluted with reducing Laemmli sample buffer, and loaded on a 7.5% (v/v) SDS−PAGE. After autoradiography, the radioactive band representing the ligand−receptor photoconjugate was excised and electroeluted from the re-swollen gel (Electro-eluter model 422, Bio-Rad) in SDS−PAGE running buffer. The electroeluted material was concentrated using Centricon 50 microconcentrators with concomitant buffer exchange to 25 mM Tris-HCl, pH 8.5, containing Triton X-100 (0.1% v/v) and SDS (0.01% v/v). The final retentate volume was 10−30 μL.

Cleavage of [^{125}I]K27−hPTH1-Rc Conjugates. All cleavage reactions were carried out at 37 °C for 24 h. The PAGE analysis of the cleavage products was performed using 16.5% Tris Tricine PAGE except for the deglycosylation of the intact receptor, which was analyzed on 7.5% SDS−PAGE.

Chemical digestions: these cleavages were carried out under N_2 in the dark. CNBr digestion was performed either (i) in solution (*26*) or (ii) on a solid support (*17*). In (i), the sample (10−30 μL) containing the radiolabled conjugate was acetone precipitated, dried, and dissolved in 70% formic acid containing 1% Triton X-100 and 0.2% SDS to which a small crystal of CNBr was added. At the end of the incubation period and prior to the PAGE analysis the sample underwent four cycles of SpeedVac drying and resuspension in water. In (ii), the sample was loaded on C18 reversed-phase silica gel columns (5000−10 000 cpm/150 mg of silica gel matrix) prewashed with methanol and equilibrated with 0.1% TFA. The column was then consecutively washed with 10 gel vol of each of the following solutions: aqueous 0.1% TFA, 0.1% TFA in acetonitrile, again with aqueous 0.1% TFA, and finally with 0.1% HCl. Incubation with 80 mg/mL CNBr in 0.1% HCl was carried out in the column. Reaction products were eluted using a stepwise gradient of 0, 20, 40, 60, 80, and 100% of 0.1% TFA in acetonitrile. Radioactive fractions were eluted at 60 and 80% acetonitrile, pooled, and concentrated for PAGE analysis.

Digestion with BNPS-skatole (5 mg/mL) was carried out in 70% acetic acid containing 1% Triton X-100 and 0.2%

SDS. PAGE analysis of the digestion mixture was preceded by treating the digestion mixture through four cycles of SpeedVac drying and resuspension in water.

Enzymatic digestions: Endo-F cleavage was carried out in 100 mM potassium phosphate buffer, pH 7.0, in the presence of 2% octyl glucoside (OG), 0.2% SDS, and 1% β-mercaptoethanol, according to the manufacturer's procedure. Lys-C and Glu-C digestions were carried out by incubating the sample of radioactive electroeluted material in 25 mM Tris-HCl buffer, pH 8.5, containing Triton X-100 (0.1% v/v) with 0.15 U of enzyme.

Receptor Mutagenesis. To modify the cleavage pattern, single point mutations were introduced into the hPTH1-Rc cDNA generating the following three mutated receptors: [L261M]-, [L261A]-, and [R262K]-PTH1Rcs. Primer pairs (sense and antisense) were prepared containing these amino acid modifications (Gibco BRL, custom primers): sense L261M (5′-to-3′), CTCACCGAGGAGGAGATGCGCGCCATCGCCCAG; sense L261A (5′-to-3′), GCCTCACCGAGGAGGAGGCGCGGGCCATCGC; and sense R262K (5′-to-3′), CACCGAGGAGGAGCTGAAGGCCATCGCCC. These primers were used in the polymerase chain reaction (PCR)-based Quik-Change site-directed mutagenesis kit (Stratagene, La Jolla, Ca) using the hPTH1-Rc in the pZeoSV2 (Invitrogen) mammalian expression vector as a template. Individual PCR reactions were used to transform TOP 10 Ultracomp cells (Invitrogen). Transformations were plated on bacteriological agar containing Zeocine. Colonies were identified and selected for plasmid isolation (Quiagen, Santa Clara, CA). Plasmid preparations were cycle sequenced (Genomix, Foster City, CA) to confirm the fidelity of mutations using oligonucleotide primers located 5′ to the regions of PTH1-Rc targeted for mutation. Each mutation was confirmed by complete sequencing.

Transient Transfection. COS-7 cells were plated at 65 000 cells/well in 24-well dishes, 24 h prior to transient transfections. Six hundred nanograms per well of either mutant or wild-type receptor cDNA constructs were transfected using 1.8 μL/well FuGENE 6 (Boehringer Mannheim) transfection reagent. Radioreceptor binding and adenylyl cyclase activity assays as well as photoaffinity cross-linking were performed 48 h after transfection as described above.

RESULTS

Bioactivity of K27 in HEK293/C-21 Cells. The design of K27 included insertion of the BP-based photophore at Lys[27], located in the principal binding domain of PTH(1−34), as well as structural modifications mandated by the PAS methodology. The latter included Met[8 & 18]-to-Nle and Trp[23]-to-2-Nal, endowing resistance toward chemical digestion by CNBr and BNPS-skatole, respectively; Lys[13 & 26]-to-Arg, endowing resistance toward Lys-C degradation; and introduction of a radioiodination site Phe[34]-to-Tyr (*20*, *24*, *26*). The resulting photoreactive analogue [Nle[8,18], Arg[13,26], L-2-Nal[23], Lys[27](N$^{\epsilon}$-*p*Bz$_2$), Tyr[34]]bPTH(1−34)NH$_2$ (K27), was bioactive. In HEK 293/C-21 cells stably overexpressing the recombinant hPTH1-Rc (400 000 Rcs/cell) (*7*), K27 displays a pharmacological profile similar to that of the parent polypeptide PTH(1−34), in terms of competing for binding of [^{125}I]PTH(1−34) [$IC_{50} = 6 \times 10^{-8}$ and $IC_{50} = 1.2 \times 10^{-8}$ nM for K27 and PTH(1−34), respectively] (Figure 1C),

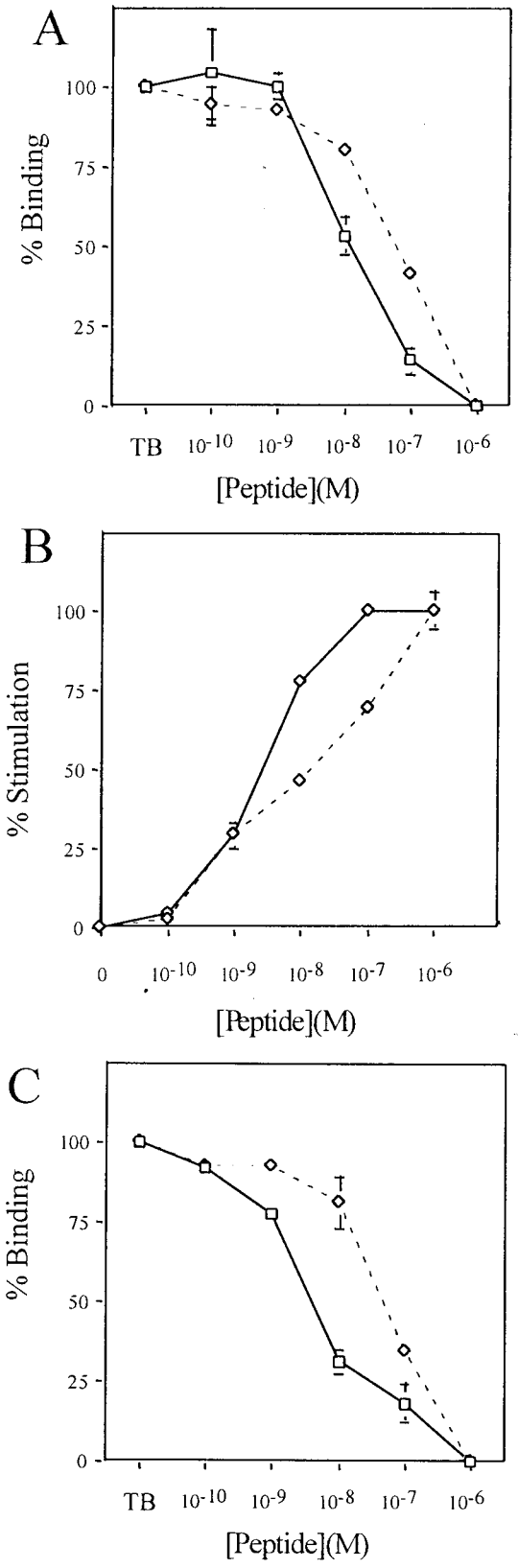

FIGURE 1: Pharmacological characterization of K27 and ^{125}I-K27 in HEK293/C-21 cells stably overexpressing the hPTH1-Rc. (A) ^{125}I-K27 binding was competitively inhibited by K27 (◇) or bPTH (1−34) (□). (B) Adenylyl cyclase activity was dose-dependently stimulated by K27 (◇) or bPTH(1−34) (□) at the indicated concentrations. (C) Binding of ^{125}I-PTH(1−34) was competitively inhibited by K27 (◇) or bPTH(1−34) (□). Average specific binding of ^{125}I-PTH(1−34) was defined as 100%. Experiments were carried out in triplicates. Curves show the mean ± SE of three independent experiments.

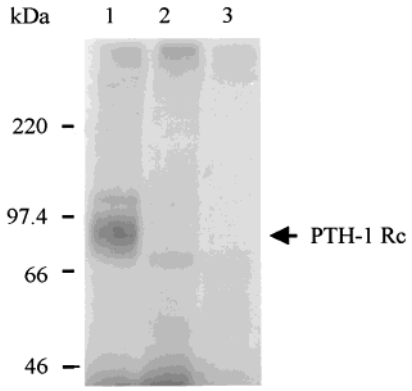

FIGURE 2: Photoaffinity cross-linking of ^{125}I-K27 to hPTH1-Rc overexpressed in HEK293/C-21 cells. ^{125}I-K27 was cross-linked to hPTH1-Rc stably expressed in HEK293/C-21 cells either alone (lane 1) or in the presence of excess (10^{-6} M) nonradiolabeled bPTH(1−34) (lane 2). Attempted cross-linking of ^{125}I-K27 to the parental nontransfected HEK 293 cells (lane 3). Samples were analyzed by SDS−PAGE (7.5%). Molecular weight markers are shown on the left. Arrow indicates position of the ∼87-kDa hormone−receptor conjugate. Data are representative of three independent experiments.

and stimulating adenylyl cyclase activity [$EC_{50} = 1.8 \times 10^{-8}$ and $EC_{50} = 2.8 \times 10^{-9}$ for K27 and PTH(1−34), respectively] (Figure 1B). Importantly, both K27 and PTH(1−34) compete for binding of ^{125}I-K27 [$IC_{50} = 4.5 \times 10^{-8}$ and $IC_{50} = 3 \times 10^{-9}$ for K27 and PTH(1−34), respectively] (Figure 1A), thus establishing the relevance and compatibility of the radioiodinated and photoreactive ^{125}I-K27 for use in PAS studies.

Photoaffinity Cross-Linking of hPTH1-Rc with ^{125}I-K27. ^{125}I-K27 cross-linked to hPTH1-Rc expressed in stably transfected HEK293/C-21 cells, yielding a single diffuse band with an apparent relative molecular mass (M_r) of ∼87 kDa on a 7.5% SDS−PAGE (Figure 2, lane 1), in agreement with the M_r values previously reported for PTH−PTH1-Rc photoconjugates (*20*, *21*, *24*, *26*, *36*). The cross-linking was specific for hPTH1-Rc inasmuch as formation of the ^{125}I-K27−hPTH1-Rc conjugate was completely inhibited in the presence of excess (10^{-6} M) unlabeled PTH(1−34) (Figure 2, lane 2). Furthermore, ^{125}I-K27 failed to cross-link to the parental nontransfected HEK 293 cells (Figure 2, lane 3), which lack the hPTH1-Rc.

Identification of a Photoinsertion Site for ^{125}I-K27 in hPTH1-Rc. The ∼87 kDa band corresponding to the ^{125}I-K27−hPTH1-Rc conjugate was isolated from the 7.5% SDS−PAGE and subjected to digestion by either CNBr or BNPS-skatole. The resultant radiolabeled ^{125}I-K27−hPTH1-Rc conjugated fragment obtained from each digestion was analyzed on 16.5% tricine/SDS−PAGE, isolated, and further digested with Glu-C. The Glu-C-generated ^{125}I-K27−hPTH1-Rc conjugated fragments were analyzed on 16.5% tricine/SDS−PAGE.

The CNBr digestion of either the glycosylated or endo-F-deglycosylated ^{125}I-K27−hPTH1-Rc conjugates (Figure 3A, lanes 1 and 2, ∼87- and ∼60-kDa bands, respectively) yielded a ∼13-kDa band (Figure 3A, lanes 3 and 5, respectively), suggesting the absence of glycosylation sites on the CNBr-derived fragment. Moreover, the electrophoretic mobility of the isolated ∼13-kDa conjugated fragment, obtained from the parent ∼87-kDa band by CNBr digestion, was not affected by Endo-F treatment (Figure 3A, lane 4), further confirming that the CNBr-restricted ^{125}I-K27−hPTH1-Rc conjugated fragment is nonglycosylated. The M_r of the receptor portion in the CNBr-derived ∼13-kDa fragment is ∼8.5 kDa (the molecular mass of ^{125}I-K27 is 4485 daltons). Analysis of the theoretical CNBr cleavage map of hPTH1-Rc reveals only one distinct nonglycosylated fragment, L^{232}−M^{312}, of molecular mass of 8961 daltons, as the putative receptor-derived domain included in the CNBr-generated ∼13-kDa band (Figure 3D). This 80-amino acid fragment includes portions of TM2 and TM3 and the entire ECL1.

A complementary fragmentation pathway of the intact ∼87-kDa ^{125}I-K27−hPTH1-Rc conjugate with BNPS-skatole (which cleaves specifically at the C-terminus of Trp residues) generated a ∼32-kDa radiolabeled conjugated fragment (Figure 3B, lane 1), which was reduced to a ∼20-kDa band following Endo F treatment (Figure 3B, lane 2). Hence, according to the theoretical BNPS-skatole-restricted digestion map, these bands represent conjugated receptor fragments of ∼27 and ∼15 kDa, corresponding to the respective glycosylated and deglycosylated (15 226 daltons) forms of hPTH1-Rc[165−298], a 134-residue sequence spanning part of the N-glycosylated N-terminal ECD, TM1, the first ICL, TM2, and part of the first ECL. Taken together, the analyses by the CNBr and the BNPS-skatole digestion pathways produce an overlapping sequence of 67 amino acids, L^{232}−W^{298} (Figure 3D).

To further identify the cross-linking site within the hPTH1-Rc[232−298], each of the isolated CNBr- and BNPS-skatole-derived conjugated fragments were subjected to a secondary digestion with endoproteinase Glu-C (which cleaves at the C-terminus of Glu residues). Unlike the digests described so far, in which the conjugated ligand remains intact, treatment with Glu-C will cleave the N-terminal sequence, [$Nle^{8,18}$, Arg^{13}]PTH(1−22) of the ligand, reducing the size of the conjugated ligand from 4485 to 1969 daltons. Importantly, this cleavage would not occur between the radiotagged residue (^{125}I-Tyr^{34}) and the conjugation site [Lys^{27}(N^{ϵ}-*p*Bz_2)], thus maintaining connectivity essential for detection during the analysis of the fragmentation pattern.

Secondary Glu-C digestions of CNBr- and BNPS-skatole-derived fragments generated ligand−receptor conjugated bands of ∼6.5 kDa apparent M_r (Figure 3C, lanes 2 and 4, respectively). According to the theoretical restriction digestion maps, these bands correspond to the respective conjugates containing the 42-amino acid fragment L^{261}−E^{302} (MW = 4578) and 38-residue stretch L^{261}−W^{298} (MW = 4124), both spanning the ECL1 (Figure 3D). Taken together, the secondary Glu-C digestions converge on an overlapping 38-amino acid hPTH1-Rc sequence, L^{261}−W^{298}.

Characterization of hPTH1-Rc Mutants Designed to Further Validate and Delineate the Sequence Containing the Photoinsertion Site. To further refine and validate the hPTH1-Rc sequence containing the insertion site for the BP moiety in ^{125}I-K27, we prepared a series of single site-directed mutations in the ECL1 portion of the receptor. The selection of mutation sites was guided toward potential insertion sites, as well as sites that would modify the pattern of CNBr- and Lys-C-restricted digestions to allow reduction of the receptor portion in the resultant conjugated fragments and to facilitate unambiguous identification. As shown in Figure 4, the L261M and R262K mutants were predicted to modify the CNBr and Lys-C cleavage pattern, respectively.

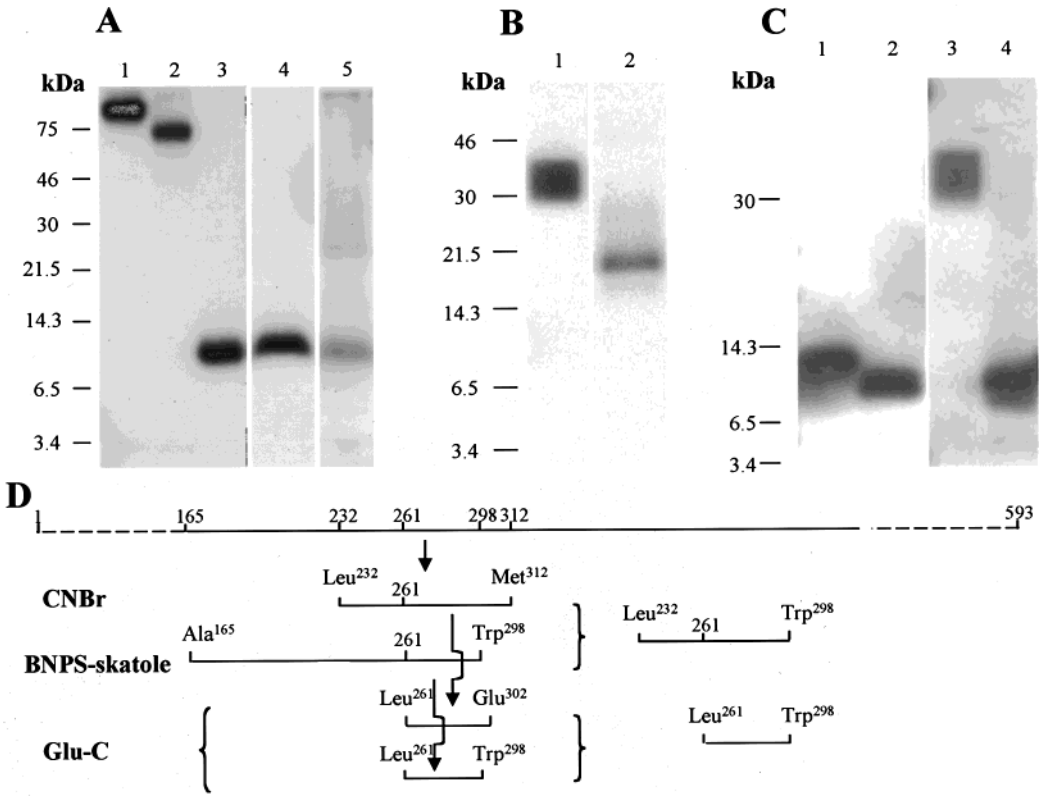

FIGURE 3: SDS−PAGE analysis of enzymatic and chemical digestions of ^{125}I-K27−hPTH1-Rc photoconjugate. (A) As described under Experimental Procedures, the isolated ~87-kDa ^{125}I-K27−hPTH1-Rc photoconjugate (lane 1) was incubated either with Endo-F yielding ~60-kDa deglycosylated ^{125}I-K27−hPTH1-Rc photoconjugate (lane 2) or CNBr generating ~13-kDa conjugated fragment (lane 3). Secondary digestions of the isolated Endo-F- and CNBr-generated bands by CNBr (lane 4) and Endo-F (lane 5), respectively. (B) Digestion of isolated ~87-kDa ^{125}I-K27−hPTH1-Rc photoconjugate with BNPS-skatole generated a ~32-kDa band, which upon treatment with Endo-F, was reduced in size to a ~20-kDa band. (C) Secondary digestions of both isolated CNBr- and BNPS-skatole-generated fragments (~13 and ~32 kDa, respectively) with Glu-C resulted in ~6.5-kDa bands. Analysis was done by 16.5% tricine/SDS−PAGE. Positions of the molecular mass markers are indicated on each figure. Data in panels A−C is representative of three similar and independent experiments. (D) Schematic presentation of the theoretical digestion map of the PTH1-Rc (top line) by the enzymatic and chemical cleavages described above (lower lines).

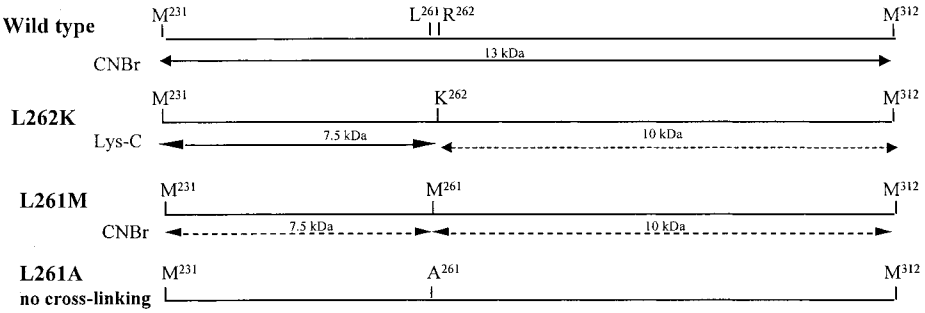

FIGURE 4: Maps of theoretical CNBr and Lys-C cleavage sites for in the point-mutated PTH1-Rc within the wild-type CNBr-generated fragment L[232]−M[312]. K[262] in [R262K]hPTH1-Rc presents a new Lys-C cleavage site, and M[262] in [L261M]hPTH1-Rc presents a new CNBr cleavage site. The potential insertion site in [L261A]hPTH1-Rc was eliminated by the point mutation in position 261. Full double-headed arrows represent photoconjugated fragments; dashed double-headed arrows represent non-crosslinked fragments. Predicted molecular mass of the CNBr- or Lys-C-generated fragments are indicated above the double-headed arrows.

The L261A mutant was introduced to eliminate a favorable insertion site at position 261.

The wild-type (wt) and mutant receptors were transiently expressed in COS-7 cells. The number of receptors expressed per cell, as determined by Scatchard analysis (data not shown), was 50 000−90 000. ^{125}I-K27 binding to the wt or each of the mutant receptors showed similar values (Table 1). In addition, PTH(1−34) stimulated adenylyl cyclase activity in cells transiently expressing either the wt (EC_{50} = 1 nM) or the different hPTH1-Rc mutants (EC_{50} range

Table 1: Pharmacological Characterization of Recombinant hPTH-1 Receptor Mutants Transiently Expressed in COS-7 Cells

receptor	binding affinity (IC_{50} in [nM])[a]	stimulation of adenylyl cyclase (EC_{50} in [nM])[b]
wild-type	1.2 ± 0.1	1 ± 0.4
L261M	2.5 ± 0.2	1 ± 0.2
L261A	3 ± 0.8	0.4 ± 0.2
R262K	0.9 ± 0.5	0.9 ± 0.3

[a] Competitive binding of [^{125}I]K27 by bPTH(1−34). [b] bPTH(1−34) stimulated adenylyl cyclase activity.

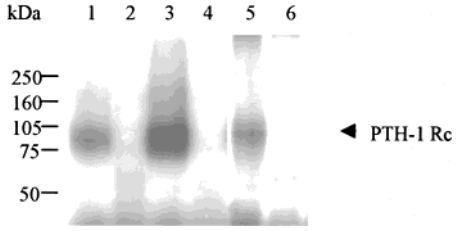

FIGURE 5: Photoaffinity cross-linking of ^{125}I-K27 to wild-type and mutant hPTH1-Rcs. Photo-cross-linking of ^{125}I-K27 to wt (lanes 1 and 2) and mutant receptors [L261M]hPTH1-Rc (lanes 3 and 4) and [R262K]hPTH1-Rc (lanes 5 and 6), transiently expressed in COS-7 cells, was performed in the absence (odd number lanes) or in the presence (even number lanes) of an excess (10^{-6} M) of nonradiolabeled bPTH(1−34). Results were analyzed by 7.5% SDS−PAGE. Positions of the molecular weight markers are shown on the left. The arrow indicates the position of the ∼87-kDa hormone−receptor conjugate. Data are representative of three similar and independent experiments.

between 0.4 and 1.2 nM) (Table 1). Taken together, the low nanomolar binding affinities and PTH(1−34)-stimulated adenylyl cyclase efficacies suggest that ligand−receptor interactions were unaffected by any of these site-specific mutations.

Photoaffinity Cross-Linking of ^{125}I-K27 to Wild-Type and Mutant hPTH1-Rcs Transiently Expressed in COS-7 Cells. Photoaffinity cross-linking of ^{125}I-K27 to transiently expressed wt and mutant [L261M]- and [R262K]hPTH1-Rcs resulted in an ∼87-kDa band similar to that observed in the cross-linking to HEK263/C-21 cells (Figure 5, lanes 1, 3, and 5, respectively). The cross-linking was receptor-specific inasmuch as it was inhibited by the presence of an excess (10^{-6} M) of nonradiolabeled PTH(1−34) (Figure 5, lanes 2, 4, and 6, respectively).

Restriction Digestion Analysis of the ^{125}I-K27. Mutant Receptor Conjugates. As predicted, CNBr digestion of the ^{125}I-K27−[R262K]hPTH1-Rc conjugate resulted in a ∼13-kDa fragment similar to the band obtained following CNBr treatment of the ^{125}I-K27−hPTH1-Rc conjugate (Figure 6A, lanes 2 and 1, respectively), which according to the above-discussed analysis corresponds to the L^{232}−M^{312} sequence (Figure 6C). However, Lys-C digestion of the isolated ∼13-kDa CNBr-generated conjugated fragment obtained from the ^{125}I-K27−[R262K]hPTH1-Rc conjugate (Figure 6B, lane 1) yielded a ∼7-kDa radiolabeled band (Figure 6B, lane 2). Analysis of the theoretical Lys-C-restriction digestion map of the CNBr-generated conjugated fragment delineated the receptor fragment containing the ^{125}I-K27 insertion site to a 31-amino acid sequence, hPTH1-Rc[232−262] (Figure 6C).

The putative photoinsertion site for Lys^{27} in PTH was isolated to a two-residue region of the PTH1-Rc by alignment of two proteolytic restriction digestion fragments. Specifically, the CNBr and BNPS-skatole restricted-digestion fragment, L^{261}−W^{298} (Figure 3D), identified in the analysis of ^{125}I-K27−hPTH1-Rc conjugate, overlaps the CNBr and Lys-C restricted-digestion fragment, L^{232}−R^{262} (Figure 6C),

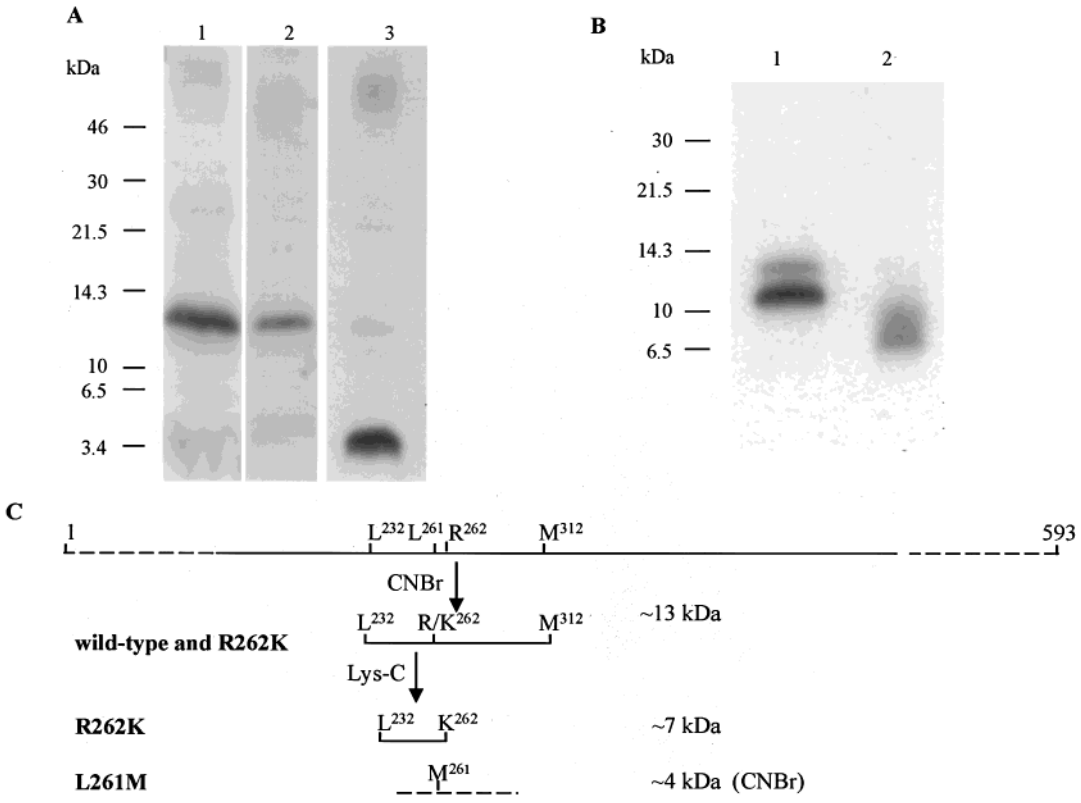

FIGURE 6: Digestion SDS−PAGE analysis of ^{125}I-K27-mutant and wild-type hPTH1-Rc photoconjugates generated in COS-7 cells. (A) Analysis of fragments generated by CNBr cleavage of the isolated ∼87 kDa ^{125}I-K27−PTH1-Rc (lane 1), ^{125}I-K27−[R262K]hPTH1-Rc (lane 2), and ^{125}I-K27−[L261M]hPTH1-Rc (lane 3) photoconjugates. (B) Secondary Lys-C digest of the ∼13-kDa excised and eluted CNBr-derived [^{125}I]K27−[R262K]hPTH1-Rc photoconjugated fragment (lane 1) generated a ∼7-kDa radiolabeled fragment (lane 2). Digests were analyzed by 16.5% tricine/SDS−PAGE. Positions of molecular mass markers are indicated on the left side of panels A and B. Data are representative of three similar and independent experiments. (C) Theoretical CNBr-restricted digestion map for the wild-type, [R262K]-hPTH1-Rc, and [L261M]hPTH1-Rc mutants and a secondary Lys-C-restricted digestion map for the CNBr-generated radiolabeled fragment obtained from [R262K]hPTH1-Rc.

identified in the analysis of the ^{125}I-K27−[R262K]hPTH1-Rc conjugate, only at residues L[261] or R[262].

CNBr cleavage of the isolated ^{125}I-K27−[L261M]hPTH1-Rc conjugate revealed a ~4-kDa radiolabeled band (Figure 6A, lane 3), which does not correspond to any of the theoretical CNBr-restricted digestion fragments. However, it is similar in size to the free ^{125}I-K27 ligand. In the absence of free ^{125}I-K27, removed prior to the excision of the ~87-kDa band (corresponding to [^{125}I]K27−[L261M]hPTH1-Rc conjugate) from the SDS−PAGE, the CNBr-generated ~4-kDa radioactive band must represent an authentic ligand−receptor conjugated fragment. Therefore, this finding suggests that cross-linking occurred on the S-CH_3 in M[261]. Upon CNBr treatment, this conjugate would yield a ligand modified by a "CH_3-SCN" moiety. This "conjugated fragment" (with CH_3-S the sole contribution from the receptor) is very similar in size to the free radioligand (*17*, *20*) and would be indistinguishable from free radioligand by SDS−PAGE.

The analyses of the photoconjugates, obtained from either the wt or the mutated hPTH1-Rcs and the ^{125}I-K27, converge consistently on position 261 in the ECL1 of hPTH1-Rc as the insertion site for the photophore presented on residue 27 in the principal binding domain of PTH(1−34).

Characterization of the [L261A]hPTH1-Rc Mutant. To address directly the role of L[261] as the putative insertion site for the BP moiety during formation of the ^{125}I-K27−hPTH1-Rc conjugate, a receptor mutant lacking this insertion site, [L261A]hPTH1-Rc, was examined. Indeed, the Leu-to-Ala substitution at position 261 completely abolished the cross-linking capacity toward ^{125}I-K27 (data not shown). Nonetheless, the mutant [L261A]hPTH1-Rc retained good binding affinity toward ^{125}I-K27 ($IC_{50} = 3 \times 10^{-9}$ M, Table 1) and very high bPTH(1−34)-stimulated adenylyl cyclase activity ($EC_{50} = 4 \times 10^{-10}$ M) (Table 1).

This result further validates the identification of L[261] (in the ECL1 of PTH1-Rc) as the complement to Lys[27] [in the principal binding domain of PTH(1−34)] at the bimolecular interface.

DISCUSSION

The present study reports on an important step in our ongoing efforts to map the bimolecular interface between PTH(1−34) and its receptor, hPTH1-Rc. The ultimate goal of these efforts is to generate an experimentally based model of the ligand−receptor complex that will provide insight into the molecular basis of the recognition and activation processes and generate a template for rationale drug design.

Unfortunately, the major advancements in sequencing and mass spectometry are not yet generally applicable to PAS studies with membrane-bound proteins, in which only minute quantities of radiolabeled conjugated material are available for analysis. In only a few studies and under special circumstances were sequencing or mass spectrometry successfully used (*17*, *37*). The PAS approach requires highly specific conjugation. In turn, this dictates that the execution of the cross-linking experiments is performed under high receptor/radioligand ratios, therefore resulting in low yield of conjugate. Additional difficulties result from low recoveries associated with hydrophobic protein derived from transmembrane domains and lack of commonly available effective affinity-based purification tools that could allow the isolation of only the conjugated receptor. The state-of-the-art in the PAS field heavily relies on the integrated analysis of multiple restricted digestions, theoretical digestion maps, and site-directed mutations (*20*−*24*, *38*−*42*).

In general, all the structural determinants necessary for expression of PTH-like in vitro and calciotropic activities in vivo are contained within the N-terminal one-third (positions 1−34) of the mature full-length PTH (*43*, *44*). Stepwise truncation from the amino terminus to the carboxyl terminus of PTH(1−34) initially generated the highly potent in vitro antagonist [Nle[8,18], Tyr[34]]PTH(3−34)NH_2 (*45*), which was later found to be a weak in vivo partial agonist (*46*). Further truncation generated [Nle[8,18], Tyr[34]]PTH(7−34)NH_2, which was devoid of any agonistic properties in vitro and in vivo (*47*), thus defining the sequence 1−6 as the "principal activation domain" of PTH. Detailed structure−activity studies indicated that the structural features of the PTH(1−34) most important for receptor binding are clustered in the carboxyl terminal 25−34 domain, which was therefore designated as the "principal binding domain" (*48*). The fragment PTH(25−34) can inhibit completely and specifically the binding of radioiodinated PTH(1−34). Taken together, PTH(1−34) represents a linear architecture in which the principal activation and binding domains are distinct and separate.

Position 27 in PTH(1−34) is centrally located in the principal binding domain, namely, residues 25−34, of the hormone. Previous results have indicated that the residues located in this domain provide the high binding affinity required for potent and specific interactions with PTH1-Rc (*45*, *48*, *49*). Substitution of Lys[27] by Thr, Met, Glu, and Ala reduced binding and activation to some extent (*50*, *51*). Interestingly, substitution of Lys[27] with Leu increases adenylyl cyclase activity (*52*) and maintains PKC activity (*53*, *54*). Furthermore, nontargeted biotinylation of PTH(1−34) suggests that acylation of Lys[27] also is tolerated (*55*, *56*). K27, in which the ϵ-amino in Lys[27] is acylated by the *p*Bz_2 moiety, is bioactive and maintains high affinity for receptor. The analogue is therefore able to serve as a photoprobe in this PAS study.

Results from enzymatic and chemical degradation of photoconjugates with wild-type and mutant hPTH1-Rcs clearly indicate L[261] as the contact point for ^{125}I-K27. The identification of L[261], located in the proximal region of ECL1 of PTH1-Rc (Figure 7), as the contact point implies intimate spatial proximity. This strongly indicates that ECL1 participates in the bimolecular ligand−receptor complex interface and contributes to hormone binding. Interestingly, ECL1 is one of the least homologous regions among the mammalian PTH1-Rcs (*57*). Previous studies, in which the ECL1 domain in PTH1-Rc was modified, suggest considerable structural latitude in the proximal region (*58*−*60*).

Substitution of E[252]−L[261] in the ECL1 of the rat (r) PTH1-Rc by the 10-amino acid (EQKLISEEDL) *c-myc* epitope was well-tolerated (*58*). Deletion of residues 258−278 in the proximal portion of ECL1 in rPTH1-Rc had a minor effect on PTH binding capacity and PTH-stimulated adenylyl cyclase response as compared to severe inactivation following the deletion of residues 284−290 in the distal portion of ECL1 (*59*). In line with these findings are studies with a rPTH1-Rc/r-secretin receptor chimera in which portions of the ECL1 domain in the rPTH1-Rc were swapped with the

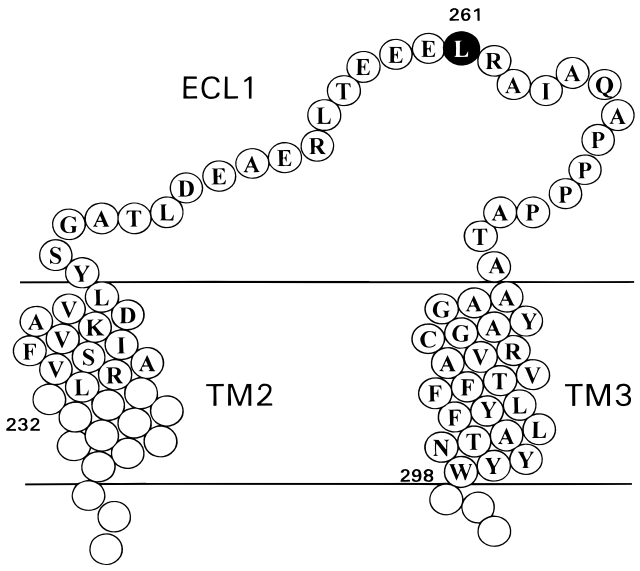

FIGURE 7: Schematic of the CNBr/BNPS-skatole fragment PTH1-Rc[232−298]. This study identifies L^{261}, in the first ECL of PTH1-Rc, as the putative contact site for Lys^{27} in the principal binding domain of PTH(1−34). CNBr cleavage, at M^{231}−L^{232}, and BNPS-skatole cleavage, at W^{298}−I^{299}, release the radiolabeled ^{125}I-K27−PTH1-Rc[232−298] photoconjugate. Identification of the boundaries of the first ECL is described elsewhere (*29*).

corresponding sequences in the r-secretin receptor (*60*). Interestingly, swapping the middle region in ECL1 of the hPTH2-Rc with homologous regions of PTH1-Rc (corresponding to residues 253−266) had no effect on ligand selectivity (*61*). However, the same manipulation in the proximal region of ECL1 (corresponding to residues 242−251 of hPTH1-Rc) had a dramatic effect on ligand specificity (*61*). The importance of ECL1 for agonist binding and selectivity in the type II subfamily of G-protein-coupled receptors was demonstrated for vasoactive intestinal polypeptide receptor (*58*, *62*), secretin receptor (*63*), and pituitary adenylate cyclase-activating polypeptide (*64*) by constructing chimeric receptors.

Recently, on the basis of a combined analysis of the [Bpa^{23}]-PTHrP(1−34)−rPTH1-Rc photoconjugate, the first 18 amino acids from the amino terminal extracellular domain were shown to include the contact site for position 23 in the ligand (*21*). It is believed that the pharmacologically equivalent and conformationally related PTH- and PTHrP(1−34)-derived agonists interact with PTH1-Rc in a similar fashion. Therefore, it is interesting to note that the adjacent positions 23 and 27 (in this study) in the ligand interact with sequentially distal sites in the receptor, the amino terminus and the ECL1, respectively. On the basis of the structural features of PTH-(1−34) (*65*), the C-terminal region of the hormone adopts an α-helix, and therefore, both positions 23 and 27 would project out in a similar direction. We hypothesize that the large extracellular amino terminus, characteristic of the type II subfamily of G-protein-coupled receptors to which PTH1-Rc belongs, and ECL1, the largest extracellular loop in PTH1-Rc, fold to generate a topology that recognizes and binds the C-terminal helix of PTH, accounting for the results from the cross-linking of the residues 23 and 27. Indeed, the accompanying article describes the structural features of a synthetic peptide comprising hPTH1-Rc(241−285) (*29*). This conformational study provides atomic insight into possible interactions between the ligand and the receptor. In this regard, the identification of L^{261} in PTH1-Rc as the contact site for Lys^{27} in PTH is particularly significant. This site is removed from the previously reported sites in PTH (namely, residues 1 and 13) and implicates ECL1, a region of the receptor not involved in the cross-linking of position 23 of PTHrP (*21*), as playing a role in ligand binding.

The significance of identifying L^{261} in PTH1-Rc as a contact site for Lys^{27} in PTH exceeds its incremental contribution to the mapping of the PTH−PTH1-Rc interface. The location of Lys^{27} and L^{261} at sites remote from previously reported interacting ligand and receptor domains generates an important additional structural constraint that can be used to upgrade and refine the emerging experimentally based model of the PTH−PTH1-Rc complex (*20*, *27*). Indeed, in the following paper in this issue (*29*), we report the integration of our findings into the PTH−PTH1-Rc model. We carried out a detailed conformational analysis (including NMR spectroscopy, distance geometry, and molecular modeling) of a synthetic peptide hPTH1-Rc(241−285) comprised from the entire ECL1 flanked by a few amino acid residues of the adjacent TM2 and TM3 (*29*). The previously generated model of the PTH−PTH1-Rc complex (*20*, *27*) was enhanced and upgraded by introducing the experimentally derived conformational features of ECL1 and the new bimolecular constraint presented by the contact between L^{261} in PTH1-Rc and Lys^{27} in the ligand.

A major finding of this report is the emergence of a bimolecular topology in which the C-terminal helix of PTH(1−34) is positioned between the first ECL and the C-terminal helix of the extracellular N-terminus of PTH1-Rc. This topological organization satisfies not only the previously reported bimolecular contacts for PTH, Lys^{13}−R^{186} (*24*, *26*) and Ser^{1}−M^{425} (*20*), but also accounts for the bimolecular interaction Lys^{27}−L^{261} reported herein. Importantly, the updated model can also accommodate the contacts between Trp^{23} in PTHrP and T^{33}/Q^{37} in PTH1-Rc (*20*).

The contact site found in this study is one of several (*20*, *21*, *24*, *26*); taken together, they form the bimolecular interface. The cumulative effect of these multisite bimolecular interactions results in specific ligand recognition, binding affinity, and eventually a conformational change in the receptor, which leads to specific intracellular signal transduction. In general, not all contact sites revealed by PAS methodology will have the same functional significance. However, all these contact sites will be part of the ligand−receptor interface and therefore indispensable targets in our mapping efforts.

REFERENCES

1. Fitzpatrick, L. A., and Bilezikian, J. P. (1996) in *Principles of Bone Biology* (Bilezikian, J. P., Raisz, L. G., Rodan, G. A., Eds.) pp 339−346, Academic Press, San Diego.
2. Segre, G. V. (1996) in *Principles of Bone Biology* (Bilezikian, J. P., Raisz, L. G., Rodan, G. A., Eds.) pp 377−403, Academic Press, San Diego.
3. Jüppner, H. (1994) *Curr. Opin. Nephrol. Hypertens. 3*, 371−378.
4. Serge, G. V., and Goldring, S. R. (1993) *Trends Endocrinol. Metab. 4*, 309−314.
5. Jüppner, H., Abou-Samra, A.-B., Freeman, M., Kong, X. F., Schipani, E., Richards, J., Kolakowski, L. F., Jr., Hock, J.,

Potts, J. T., Jr., Kronenberg, H. M., and Segre, G. V. (1991) *Science 254*, 1024−1026.
6. Pines, M., Fukayama, S., Costas, K., Meurer, E., Goldsmith, P. K., Xu, X., Muallem, S., Behar, V., Chorev, M., Rosenblatt, M., Tashjian, A. H., Jr., and Suva, L. J. (1996) *Bone 18*, 381−389.
7. Pines, M., Adams, A. E., Stueckle, S., Bessalle, R., Rashti-Behar, V., Chorev, M., Rosenblatt, M., and Suva, L. J. (1994) *Endocrinology 135*, 1713−1716.
8. Abou-Samra, A.-B., Jüppner, H., Force, T., Freeman, M. W., Kong, X.-F., Schipani, E., Urena, P., Richards, J., Bonventre, J. V., Potts, J. T., Jr., Kronenberg, H. M., and Segre, G. V. (1992) *Proc. Natl. Acad. Sci. U.S.A. 89*, 2732−2736.
9. Chorev, M., and Rosenblatt, M. (1994) in *The Parathyroids* (Bilezikian, J. P., Levine, M. A., and Marcus, R., Eds) pp 139−156, Raven Press, Ltd., New York.
10. Williams, K. P., and Shoelson, S. E. (1993) *J. Biol. Chem. 268*, 5361−5364.
11. Dorman, G., and Prestwich, G. D. (1994) *Biochemistry 33*, 5661−5673.
12. Kojro, E., Eich, P., Gimpl, G., and Fahrenholz, F. (1993) *Biochemistry 32*, 13537−13544.
13. Blanton, M. P., Li, Y. M., Stimson, E. R., Maggio, J. E., and Cohen, J. B. (1994) *Mol. Pharmacol. 46*, 1048−1055.
14. Keutmann, H. T., and Rubin, D. A. (1993) *Endocrinology 132*, 1305−1312.
15. Li, Y. M., Marnerakis, M., Stimson, E. R., and Maggio, J. E. (1995) *J. Biol. Chem. 270*, 1213−1220.
16. Boyd, N. D., Kage, R., Dumas, J. J., Krause, J. E., and Leeman, S. E. (1996) *Proc. Natl. Acad. Sci. U.S.A. 93*, 433−437.
17. Kage, R., Leeman, S. E., Krause, J. E., Costello, C. E., and Boyd, N. D. (1996) *J. Biol. Chem. 271*, 25797−25800.
18. Girault, S., Sagan, S., Bolbach, G., Lavielle, S., and Chassaing, G. (1996) *Eur. J. Biochem. 240*, 215−222.
19. McNicoll, N., Gagnon, J., Rondeau, J.-J., Ong, H., and De Lean, A. (1996) *Biochemistry 35*, 12950−12956.
20. Bisello, A., Adams, A., Mierke, D. F, Pellegrini, M., Rosenblatt, M., Suva, L., and Chorev, M. (1998) *J. Biol. Chem. 273*, 22498−22505.
21. Mannstadt, M., Luck, M., Gardella, T., and Jüppner, H. (1998) *J. Biol. Chem. 273*, 16890−16896.
22. Behar, V., Bisello, A., Rosenblatt, M., and Chorev, M. (1999) *Endocrinology 140*, 4251−4261.
23. Behar, V., Bisello, A., Rosenblatt, M., and Chorev, M. (2000) *J Biol. Chem. 275*, 9−17.
24. Adams, A. E., Bisello, A., Chorev, M., Rosenblatt, M., and Suva, L. J. (1998) *Mol. Endocrinol. 12*, 1673−1683.
25. Chorev, M., and Rosenblatt, M. (1996) in *Principles of Bone Biology* (Bilezikian, J. P., Raisz, L. G., Rodan, G. A., Eds.) pp 305−323, Academic Press, Inc., San Diego.
26. Zhou, A. T., Besalle, R., Bisello, A., Nakamoto, C., Rosenblatt, M., Suva, L. J., and Chorev, M. (1997) *Proc. Natl. Acad. Sci. U.S.A. 94*, 3644−3649.
27. Rolz, C., Pellgrini, M., and Mierke, D. F. (1999) *Biochemistry 38*, 6397−6405.
28. Rosenblatt, M., Segre, G. V., Tyler, G. A., Shepard, G. L., Nussbaum, S. R., and Potts, J. T., Jr. (1980) *Endocrinology 107*, 545−550.
29. Piserchio, A., Bisello, A., Rosenblatt, M., Chorev, M., and Mierke, D. F. (2000) *Biochemistry 39*, 8153−8160.
30. Merrifield, R. B. (1963) *J. Am. Chem. Soc. 85*, 2149−2154.
31. Nakamoto, C., Behar, V., Chin, K. R., Adams, A. E., Suva, L. J., Rosenblatt, M., and Chorev, M. (1995) *Biochemistry 34*, 10546−10552.
32. Goldman, M. E., Chorev, M., Reagan, J. E., Nutt, R. F., Levy, J. J., and Rosenblatt, M. (1988) *Endocrinology 123*, 1468−1475.
33. Roubini, E., Duong, L. T., Gibbons, S. W., Leu, C. T., Caulfield, M. P., Chorev, M., and Rosenblatt, M. (1992) *Biochemistry 31*, 4026−4033.
34. Solomon, Y., Londos, C., and Rodbell, M. A. (1974) *Anal. Biochem. 58*, 541−548.
35. Laemmli, U. K. (1970) *Nature 227*, 680−685.
36. Adams, A. E., Pines, M., Nakamoto, C., Behar, V., Yang, Q. M., Besalle, R., Chorev, M., Rosenblatt, M., Levine, M. A., and Suva, L. J. (1995) *Biochemistry 34*, 10553−10559.
37. Girault, S., Chassaing, G., Blais, J. C., Brunot, A., and Bolbach, G. (1996) *Anal. Chem. 68*, 2122−2126.
38. Phalipou, S., Seyer, R., Cotte, N., Breton, C., Barberis, C., Hibert, M., and Mouillac, B. (1999) *J. Biol. Chem. 274*, 23316−27.
39. Dong, M., Wang, Y., Pinon, D., Hadac, E., and Miller, L. (1999) *J. Biol. Chem. 274*, 903−909.
40. Servant, G., Laporte, S. A., Leduc, R., Escher, E., and Guillemette, G. (1999) *J. Biol. Chem. 272*, 8653−8659.
41. Hadac, E. M., Ji, Z., Pinon, D. I., Henne, R. M., Lybrand, T. P., and Miller, L. J. (1999) *J. Med. Chem. 42*, 2105−2111.
42. Kotzyba-Hibert, F., Grutter, T., and Goeldner, M. (1999) *Mol. Neurobiol. 20*, 45−59.
43. Potts, J. T., Jr., Tregear, G. W., Keutmann, H. T., Niall, H. D., Sauer, R., Deftos, L. J., Dawson, B. F., Hogan, M. L., and Aurbach, G. D. (1971) *Proc. Natl. Acad. Sci. U.S.A. 68*, 63−67.
44. Tregear, G. W., van Rietschoten, J., Greene, E., Keutmann, H. T., Niall, H. D., Reit, B., Parsons, J. A., and Potts, J. T., Jr. (1973) *Endocrinology 93*, 1349−1353.
45. Rosenblatt, M., Callahan, E. N., Mahaffey, J. E., Pont, A., and Potts, J. T., Jr. (1977) *J. Biol. Chem. 252*, 5847−5851.
46. Horiuchi, N., Rosenblatt, M., Keutmann, H. T., Potts, J. T., Jr., and Holick, M. R. (1983) *Am. J. Physiol. 244*, E589−E595
47. Horiuchi, N., Holick, M. F., Potts, J. T., Jr., and Rosenblatt, M. (1983) *Science 220*, 1053−1055.
48. Nussbaum, S. R., Rosenblatt, M., and Potts, J. T., Jr., (1980) *J. Biol. Chem. 255*, 10183−10187.
49. Caulfield, M. P., McKee, R. L., Goldman, M. E., Duong, L. T., Fisher, J. E., Gay, C. T., DeHaven, P. A., Levy, J. J., Roubini, E., Nutt, R. F., Chorev, M., and Rosenblatt, M. (1990) *Endocrinology 127*, 83−87.
50. Gardella, T. J., Wilson, A. K., Keutmann, H. T., Oberstein, R., Potts, J. T., Jr., Kronenberg, H. M., and Nussbaum, S. R. (1993) *Endocrinology 132*, 2024−2030.
51. Gombert, F. O., Games, R., Feyen, J. H. M., and Cardinaux, F. (1996) in *Peptides: Chemistry, Structure and Biology* (Kaumaya, P. T. P., Hodges, R. S., Eds.) pp 661−662, Mayflower Scientific Ltd., England.
52. Barbier, J.-R., Neugebauer, W., Morley, P., Ross, V., Soska, M., Whitfield, J. F., and Willick, G. (1997) *J. Med. Chem. 40*, 1373−1380.
53. Neugebauer, W., Gagnon, L., Whitfield, J., and Willick, G. E. (1994) *Int. J. Pept. Protein Res. 43*, 555−562.
54. Surewicz, W. K., Neugebauer, W., Gagnon, L., MacLean, S., Whitfield, J. F., and Willick, G. (1994) in *Peptides, Chemical Structures and Biology* (Hodges, R. S., Smith, J. A., Eds) pp 556−558, ESCOM, Leiden.
55. Newman, W., Beall, L. D., Levine, M. A., Cone, J. L., Randhawa, Z. I., and Bertolini, D. R. (1989) *J. Biol. Chem. 264*, 16359−16366.
56. Abou-Samra, A.-B., Freeman, M., Jüppner, H., Uneno, S., and Segre, G. V. (1990) *J. Biol. Chem. 265*, 58−62.
57. Schipani, E., Karga, H., Karaplis, A. C., Potts, J. T., Jr., Kronenberg, H. M., Segre, G. V., Abou-Samra, A.-B., and Jüppner, H. (1993) *Endocrinology 132*, 2157−2165.
58. Olde, B., Sabirsh, A., and Owman, C. (1999) *J. Mol. Neurosci. 11*, 127−134.
59. Lee, C., Gardella, T. J., Abou-Samra, A.-B., Nussbaum, S. R., Segre, G. V., Potts, J. T., Jr., Kronenberg, H. M., and Jüppner, H. (1994) *Endocrinology 135*, 1488−1495.
60. Lee, C., Luck, M. D., Jüppner, H., Potts, J. T., Jr., Kronenberg, H. M., and Gardella, T. J. (1995) *Mol. Endocrinol. 9*, 1269−1278.
61. Bergwitz, C., Jusseaume, S. A., Luck, M. D., Jüppner, H., and Gardella, T. J. (1997) *J. Biol. Chem. 272*, 28861−28868.

62. Holtmann, M. H., Hadac, E. M., and Miller, L. J. (1995) *J. Biol. Chem. 270*, 14394−14398.
63. Holtmann, M. H., Ganguli, S., Hadac, E. M., Dolu, V., and Miller, L. J. (1999) *J. Biol. Chem. 271*, 14944−14949.
64. Hashimoto, H., Ogawa, N., Hagihara, N., Yamamoto, K., Imanishi, K., Nogi, H., Nishino, A., Fujita, T., Matsuda, T., Nagata, S., and Baba, A. (1997) *Mol. Pharmacol. 52*, 128−135.
65. Pellegrini, M., Royo, M., Rosenblatt, M., Chorev, M., and Mierke, D. F. (1998) *J. Biol. Chem. 273*, 1565−1585.

BI000195N